Direct electron attachment to fast hydrogen in 10^{-9} contrast 10^{18} Wcm^{-2} intense laser solid target interaction

Direct electron attachment to fast hydrogen in 10^{-9} contrast 10^{18} Wcm^{-2} intense laser solid target interaction

Sheroy Tata[1], Angana Mondal[1], Soubhik Sarkar[1], Amit D. Lad[1], James Colgan[2], John Pasley[3] and M. Krishnamurthy[1,4]

[1]Tata Institute of Fundamental Research, Mumbai 400 005, India
[2]Los Alamos National Laboratory, New Mexico 87544, USA
[3]York Plasma Institute, Department of Physics, University of York, York, YO10 5DD, United Kingdom
[4]TIFR Centre for Interdisciplinary Sciences, Hyderabad 500 075, India

E-mail: mkrism@tifr.res.in

Abstract. The interaction of an ultra-short (<30 fs), high-contrast($<10^{-9}$), high-intensity ($>10^{18}$ Wcm^{-2}) laser pulse with a solid target is not generally known to produce and accelerate negative ions. The transient accelerating electrostatic-fields are so strong that they ionize any atom or negative ion at the target surface. In spite of what may appear to be unfavourable conditions, here it is reported that H^- ions extending up to 80 keV are measured from such an interaction. The H^- ion flux is about 0.1% that of the H^+ ions at 20 keV. These measurements employ a recently developed temporally-gated Thomson parabola ion spectrometry diagnostic which significantly improves signal-to-noise ratios. Electrons that co-propagate with the fast protons cause a two-step charge-reduction reaction. The gas phase three-body attachment of electrons to fast neutral hydrogen atoms accounts for the measured H^- yield. It is intriguing that such a fundamental gas-phase reaction, involving the attachment of an electron to a hydrogen atom, has not been observed in laboratory experiments previously. Laser-produced plasma offers an alternative environment to the conventional charged particle beam experiments, in which such atomic physics processes can be investigated.

1. Introduction

H^- is one of the simplest bound three-particle systems, and it is important for both fundamental and applied research. As the simplest model system for electron correlations and the study of the fundamental properties of negative ions, it has drawn considerable attention [1, 2]. Electron attachment to H^0 may appear to be an easy way of generating H^-, but actually this is one of the least studied of the electron attachment reactions. Almost all of the laboratory techniques for generating H^- ions [3, 4] are either through charge-transfer reactions on surfaces coated with electro-positive atoms such as Cs [5] or in molecular fragmentation schemes [6]. H^- is also of interest for plasma heating in Tokamak reactors. Negative ions are crucial in conventional tandem accelerators where they offer the possibility to derive maximum energy from the electrostatic potentials applied in the acceleration columns [7]. Hybrid approaches which combine laser-plasma acceleration with conventional methods have recently been explored [8]. The possibility of generating negative ions from a laser-plasma accelerator could be of interest from such a perspective.

To the best of our understanding, a direct chain of recombination reactions where protons are reduced to H^- in gas phase beam experiments has not been reported thus far. Indeed, the absence of reported reaction rates for the reduction of H^0 to H^- with electrons has meant that it was necessary to compute the relevant electron attachment rates in order to model the experiments presented here. Impulsive excitation of matter by ultra-short laser pulses raises the electron temperature rapidly in a few tens of femtoseconds. The temperature then falls off again over a period of nanoseconds. During the excitation, high-brightness electron pulses stream out of the focal spot and generate extraordinarily high rates of ionization, excitation and even recombination (as has been recently evidenced in reference 9). Intense-laser produced plasma thus offers an environment in which atomic-physics experiments that probe such fundamental atomic processes can be performed. In this manuscript we describe observations of the elusive gas-phase reduction of fast H^0 atoms to form fast H^- ions in a laser-produced plasma experiment in which dense bunches of electrons and ions co-propagate.

Intense ($\geq$ 10^{18} W cm^{-2}), ultra-short ($\leq$ 100 fs) laser pulses incident on a solid target are known to accelerate $\sim$ MeV ions [10, 11, 12, 13] from the target surface. Electrons absorb energy from the incident light by various mechanisms. This produces a high temperature electron distribution that can extend to a few hundred keV [14] while the bulk thermal electron population is also raised to temperatures of up to a few hundred electron-volts [15, 16]. Since the target is heated by the high-contrast short laser-pulse, the ions remain relatively immobile during the laser interaction due to their large mass. On the other hand, electrons are removed far from the target surface and this results in a transient charge separation field that can be as high as $100-1000$ GV/m depending on the laser intensity and pulse duration [17]. Over time, this field energy is transferred to the positive ions and they are accelerated along the target normal. Surface contaminants, typically hydrocarbon impurities, are typically the principle source of the

accelerated positive ions. Protons, having the lowest mass to charge ratio are accelerated most vigorously. Proton energies extending to MeV (and higher for more intense lasers) are studied not only to devise new acceleration schemes [18] but also to understand the generation mechanism [17] and the evolution of the hot, dense plasma. One rarely finds discussion of negative-ion formation or acceleration in such sheath-field ion-acceleration schemes.

Negative ion formation has been reported in a few intense laser plasma experiments in the past, with the underlying mechanism suggested to be charge-transfer collisions with neutral atoms. The relatively high neutral atom density along the path of the ion beam, or surrounding the laser focus, has enabled the charge transfer mechanism in all of these previous experiments. In special targets, such as liquid droplet sprays [19, 20, 21, 22] or nanoclusters [23, 24, 25] the large cross-sections for charge transfer processes were shown to be responsible for the negative ion formation. Negative ion formation has been reported from solid targets when the pulse duration is large [26, 27], or when the pulse contrast is poor [28], due to collisions with neutrals in the ablation plume. In a recent study [28], negative ion formation is observed when the laser is focused deep inside a transparent PMMA target. Here the charge transfer from C or O atoms appear to be the main reason for the negative ion formation.

Recently, we have shown [9] that laser-plasma based particle acceleration of ions is not just limited to the three steps of a) ejection of hot electrons, b) setting up of transient electrostatic fields and c) ion acceleration. The process of ion acceleration also leads to the ejection of low energy electrons. It is well known that a fraction of these electrons have the same velocity as that of the accelerated ions and co-propagate with them [29, 30, 9]. This situation is different from the quasi-neutralilty in a plasma. Here ions and electrons travel toward the detector with their terminal velocities. A few tens of mm away from the target, the electron density is very low such that the individual particle interactions tend to dominate collective behaviour. In such a regime, the interaction between the co-propagating electrons and ions continues long after the ions leave the hot dense plasma. During this time, electron-ion recombination reduces the proton population and produces a substantial fraction of fast neutral hydrogen atoms. Extensive experiments have been performed to demonstrate this behaviour, including changing the pulse energy and pulse duration, pump-probe studies, and pinhole imaging of the neutral spot on the detector. Here we show that such co-propagation reactions are not limited to producing fast neutral hydrogen atoms, but can also result in the formation of negative ions.

In this paper, we report H^- generation up to 80 keV when a high intensity ($\geq 10^{18}$ W/cm^2), high contrast (10^{-9}) laser pulse irradiates the surface of a target. Under these high-contrast conditions, neither charge transfer with neutral atoms nor electron-ion recombination with a single electron is sufficient to explain the formation of negative ions. Charge reduction of the accelerated ions is shown to occur by direct interaction with the dense bunch of electrons that is co-propagating with them. It is demonstrated that the two-step electron recombination and attachment reactions with

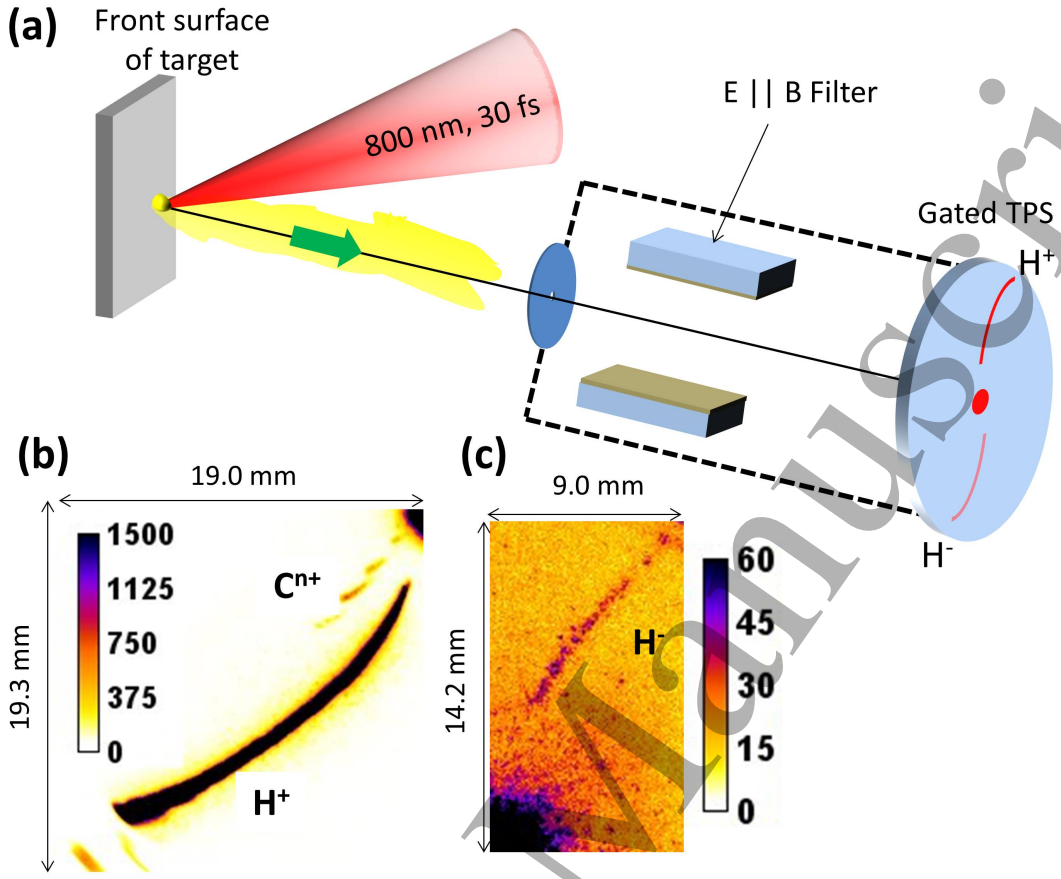

Figure 1. (a) A schematic of the experimental set-up where the MCP is gated to switch on only during the arrival time of H. (b) The TPS trace shows the enhanced view of the quadrants where H^+ and carbon ions are seen. (c) In the diagonally opposite quadrant a clear parabolic trace of H^- is also seen.

protons are responsible for the generation of the fast H^- ions observed.

2. Experiment

An 800 nm, 30 fs laser with an energy of $\approx$ 1.2 J on target and a spot size of 13 μm FWHM is used to obtain a peak focused intensity of $\approx 1.5 \times 10^{19}$ W/cm^2. The angle of incidence was kept at 45° with p-polarization. The target consisted of a 5 mm thick substrate with a few tens of nanometers thick Al coating on BK-7 glass. The metal target should be $\lambda/10$ polished and the easiest way to get a metal target of such smoothness is to use a $\lambda/10$ polished BK-7 glass target coated with Al of thickness larger than the skin depth of the laser. The laser was irradiated on the coated surface of the target and backward accelerated target normal ions are characterized using a Thomson parabola spectrometer (TPS) placed along the target normal direction. A micro-channel plate (MCP) coupled with a phosphor screen is used as the detector in the TPS which is

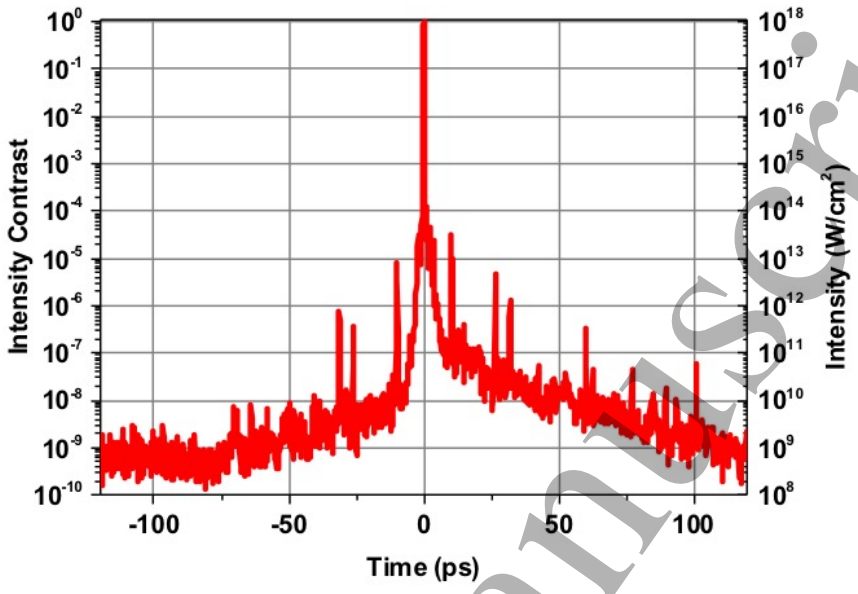

Figure 2. Third-order autocorrelation measurement showing the intensity contrast of the laser pulse used in the experiments. The ns contrast of the pulse is better than 10^{-9}. Picosecond contrast is in the range of 10^{-7} to 10^{-5}.

imaged by a 12-bit CCD camera to record the signal. The MCP has a provision to be controlled by a fast electronic switch to detect ions of a particular species based on the ion arrival time [31]. To optimize the dynamic range in energy and the signal to noise ratio a gate delay of approximately 50 ns and a gate width of 1.1 μs is used. A schematic of the set-up is shown in Fig. 1(a). The accelerated ions propagate through a vacuum of 9×10^{-5} mbar for 63 cm followed by another evacuated region at 7×10^{-7} mbar for 73 cm before they reach the detector.

It is well known that laser pulse contrast plays a key role in determining both the absorption and ion acceleration mechanisms that occur in a given laser:solid-target interaction. Low levels of pulse contrast can lead to a larger scale length plasma and a diminished sheath potentials. The presence of a large prepulse causes ablation of the target surface and consequent hydrodynamic modification of the target geometry and properties; it also increases the fraction of low-energy electrons produced. In order to gain a better understanding of the physics of the laser-target interaction in these experiments, the pulse contrast is measured and this measurement is used to provide input parameters for radiation-hydrodynamics simulations. The goal of these simulations is to predict the temperature and density profiles in the plasma column in which the protons move as they propagate out toward the detector. We use a third-order autocorrelator to measure the pulse contrast of the laser pulse. Fig.2 gives the measured pulse-contrast. We do not have any other pre-pulse in the experiment and the ns pre-pulse is measured to be $<10^{-9}$.

3. Results and Discussion

Our recently devised gated Thomson-parabola spectrometry for ions diagnostic has significantly improved the achievable signal-to-noise ratio (SNR) in our measurements [31]. Low-yield ion signals in the experiments carried out previously, in absence of such a diagnostic, may have escaped detection [31]. With this improved capability, not only is the routinely observed H^+ trace seen, but also a clear parabolic trace due to H^- is recorded in the opposite quadrant. The TPS traces in both quadrants are shown in Fig 1(b, c), when the acquisition window is set to the arrival time of the protons. The energy spectrum of the H^+ and H^- ions derived from the parabolic traces are shown in Fig. 3. The procedure for converting the TPS image to the energy spectrum, along with the noise corrections, is explained in detail in our recent work[32]. It is seen that the proton spectrum at the back of a thin foil extends to a few MeV, but for a thick target on the side upon which the laser is incident, the blow-out plasma limits maximum energy, even though the experiments are done with high contrast pulses [33, 34]. The flux of H^- ions relative to the H^+ flux is about 0.1 % at 20 keV. It is to be noted that for the H^- spectrum, the flux drops sharply at ≈ 80 keV, whilst the H^+ spectrum continues further and falls off at a distinct cut-off defined by the accelerating potential of about 180 keV. This shows that even when a simple solid target is used with a high contrast, high intensity, ultra-short laser pulse, the generation of fast negative hydrogen ions occurs. The possible generation mechanisms of these negative ions will now be considered in detail.

The electronic binding energy of the H^- ion is $\approx$ 0.75 eV [35] and requires an electric field of only $\approx$ 90 MV/m in order to remove the extra bound electron. Much larger electric fields are generated in the ion acceleration phase at the target surface and such fields would immediately auto-ionize the negative ions. In the event that the negative ions are not auto-ionized, the target normal sheath acceleration process would accelerate such negative ions into the target surface and not away from the target.

The only available process for fast negative ion formation is therefore multiple charge reduction of the accelerated positive ions. The proton acceleration mechanism in this conventional laser:solid-target system is thought to be due to the well studied TNSA process[13, 17]. The laser-plasma interaction causes electrons to be accelerated to relativistic velocities and to escape the target. As these hot electrons move away from the target, a sheath field is generated, which in turn accelerates protons (and other heavier ions). Since this ion-acceleration mechanism has already been subject to extensive investigation and has been well demonstrated in the existing literature, the focus here will be to try and explain the possible charge reduction physics that generates the negative ions. The two main processes of charge reduction are either by: a) capture of a free electron; this process is termed conventionally as electron-ion recombination, or b) the capture of electrons from bound states of other atomic systems, conventionally termed electron capture/charge transfer. Bound electron capture generally occurs via collisions with neutral atoms [36]. One of the electron-ion recombination mechanisms is

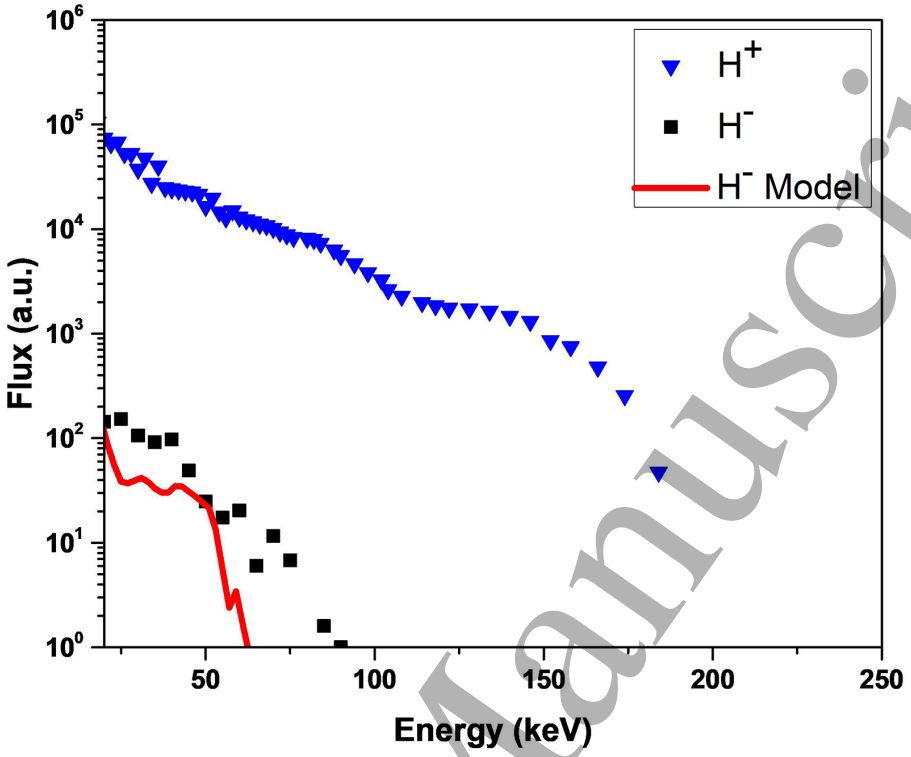

Figure 3. Ion spectra of protons and negative ions. The proton spectrum has a cut-off at about 180 keV while for the negative ions, the spectrum becomes undetectable much above 80 keV. The red line shows the computed H^- spectrum based on the co-propagation scheme of electrons of similar velocity interacting with the ions far away from the target (few mm) and undergoing three-body recombination to form H^-.

a three-body process where two electrons simultaneously interact with the ion[37]. One of the electrons is captured by the ion in to the ground state and the other electron is scattered to conserve the momentum.

Before we discuss these processes in detail, it is important to evaluate the possibility of charge reduction by means charge transfer reactions between the accelerated protons and the background gas. The cross section of charge transfer of H^+ to H^0 from the background gas is 6×10^{-16} cm^2 at 10 keV [38] and for a second electron capture to form H^-, it is $\approx 1.5 \times 10^{-17}$ cm^2 [38]. For our experimental conditions of 9×10^{-5} mbar chamber pressure and 63 cm of traversal, it is estimated that the charge transfer probability to generate H^- at 20 keV is $\approx$ 0.01 % while the experiments yield is about 0.1 %. So charge transfer due to the background gas is able to account for at most a tenth of the signal measured and is therefore unable explain the experimental measurements. Charge transfer collisions with neutral atoms formed in ablative emission or in the plasma plume are also a possibility that needs to be evaluated. Protons being least massive and the first ions to move out, they will be ahead of any ablative neutral emission and electron capture from these particles is not feasible.

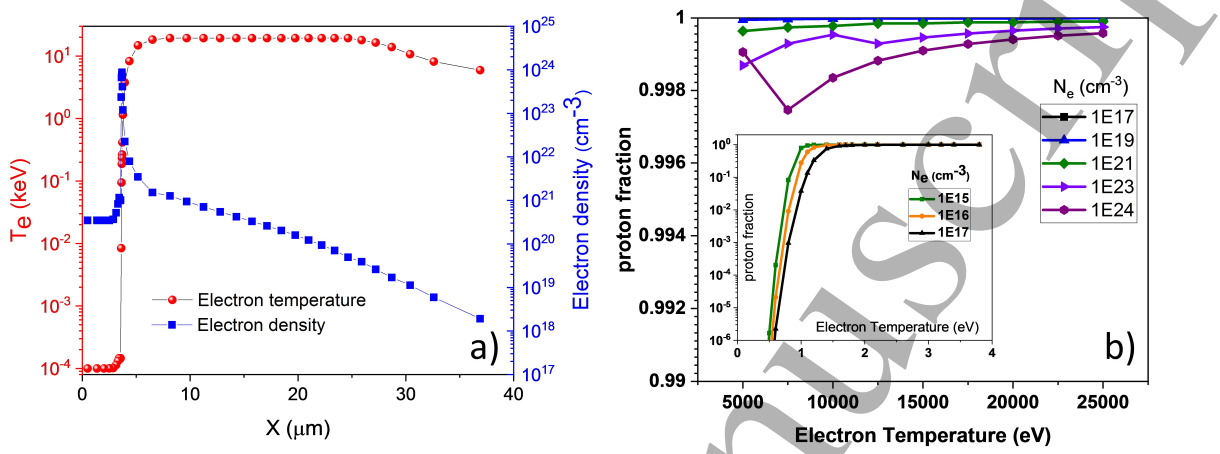

Figure 4. (a) The electron temperature and density profiles close to the target surface 1 ps after the laser-target interaction taken from HYADES radiation-hydrodynamics simulation results. (b) The proton fraction in the plasma computed for different electron densities and temperatures using FLYCHK. Unless the electron temperature is less than 2eV electron-ion recombination is small and the proton fraction remains close to 1.

All charge reduction processes by free electron attachment intrinsically require low electron temperature so that re-ionization of a neutral atom in the presence a swarm of free electrons is avoided. At distances close to the surface of the target, within a few tens of μm, the plasma temperature is expected to be very high and the neutral atom density under such conditions may be negligibly low to contribute to the charge transfer process. Effective charge reduction by electron-ion recombination demands that the electron density be high but more importantly requires that the electron temperature should be at most a few electron volts. For example, in the case of electron capture by Argon ions, the total electron-ion recombination cross-section decreases by four orders of magnitude if the electron energy increases from $1 - 10$ eV [39]. The decline in the cross section is even larger for electron energies above 10 eV. Thus, charge reduction by electron-ion recombination to form fast neutral hydrogen is effective only when the electron temperature falls below 1 eV. Three-body recombination provides another possibility of charge reduction, whereby two electrons interact simultaneously with a positive ion to capture an electron. This also requires that the electron density be very high, but this is only possible when the electron temperature is low, typically 1 eV or less, so as to prevent re-ionization of the H^-.

It is important to evaluate the first charge reduction step to form neutral H that must occur as a precursor to negative ion formation. This requires a detailed analysis of the density and temperature and how these parameter change with time. We also need to evaluate how the neutralisation changes for a given parameter space of electron

density and temperature. A one-dimensional radiation hydrodynamics simulation using HYADES [40] is used, along with calculations performed using the FLYCHK [41] and ATOMIC [42, 43] codes, to support this analysis. HYADES is used to calculate the plasma scale-length and temperature near the target surface 1 ps after the laser pulse. 1 ps is chosen since this is the typical time taken for the protons to be accelerated from the target. The electron density and temperature profiles obtained are shown in Fig. 4(a). For the Al target, it was found that all atoms near the target front surface are fully ionized (upto a few few tens of μm), with an average charge state of 13. This negates the possibility that H^- is forming in this region via electron capture; the neutral population is negligible.

Steady state electron-ion recombination rates are calculated to compute the average charge of the proton bunch moving out of the plasma using FLYCHK. For the electron density and temperatures shown in Fig. 4(a) there is practically no charge reduction. Inset shows that charge reduction is possible even at low densities when the electron temperature is low. Unless the electron temperatures fall as low as 2eV there is no effective electron-ion recombination and the proton fraction remains unchanged. The question then is whether the electron energies in the vicinity of the target can fall to such low values in the time taken for the protons to move out of the target vicinity. To determine this we refer to the hydrodynamic simulation results. HYADES computed electron temperatures in the low-density plasma are in the keV range (Fig. 4a) and remain so even after 25ps as shown in Fig. 5. Even in the higher density portion of the plasma the temperatures are typically a few hundred eV. This is clearly too high to allow for any effective electron-ion recombination in the species of interest. Fig. 5 also establishes that even after 25 ps, the charge state of the Al is very high such that any possible charge reduction by charge transfer collisions is not possible. We present FLYCHK computations over a large range of parameters to make it clear that irrespective of the plasma density or any reasonable plasma temperature, even a single-step charge reduction to form neutral hydrogen is unlikely, let alone the consecutive second reaction to reduce H^0 to H^-.

In our recent study on fast hydrogen atom generation from intense laser pulses interacting with solid targets [9], it was seen that fast hydrogen atoms are generated by electron-ion recombination where low energy electrons co-propagating with protons interact over an extended distance, far away from the target (few mm). As the ions are accelerated from the target, the potential of the accelerating field drops and more low energy electrons can be released. A fraction of these electrons have the same velocity of the ions and undergo recombination reactions to form fast neutral atoms [9]. The negative ions seen here can only be produced by a similar scheme given that all the other possibilities have been ruled out. Further studies have been carried out to evaluate if the presence of these co-propagating electrons with protons can result in two-step recombination and attachment reactions to form negative ions.

Toward this end, recombination rates for the reduction of neutral hydrogen to H^- are needed. Although measurements and calculations exist for electron-impact

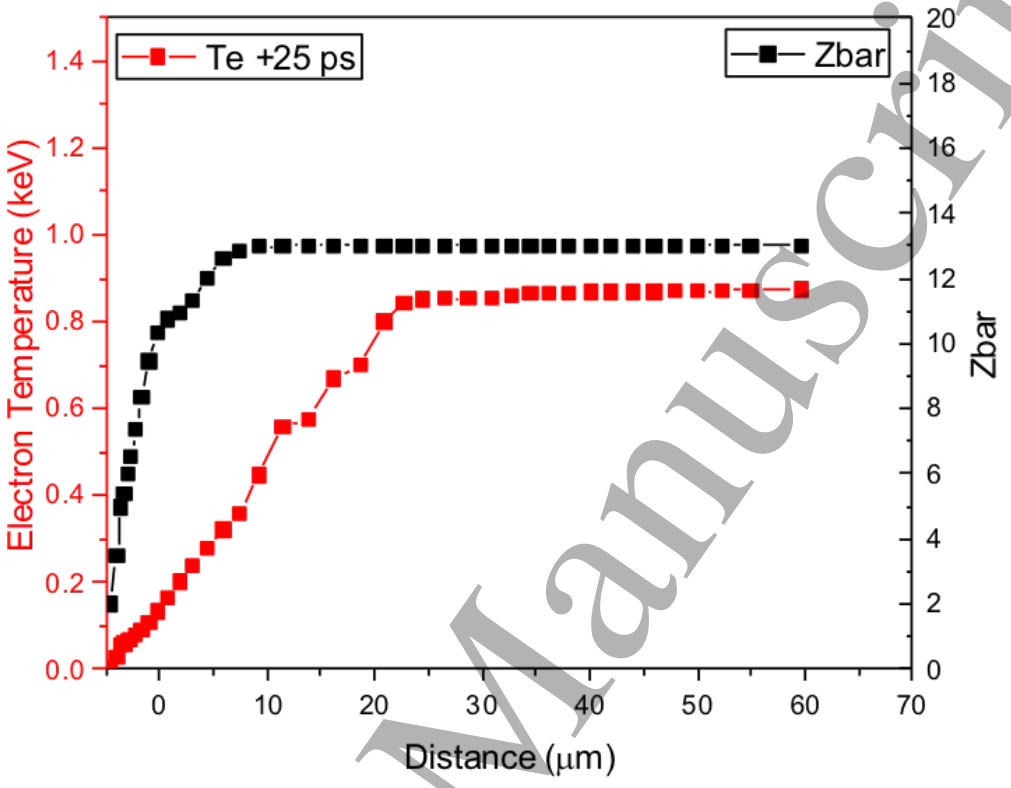

Figure 5. (a) Electron temperature and density profile close to the target surface at 25 ps after the laser pulse is incident on the target as computed using the HYADES 1D radiation-hydrodynamics simulation code. Though electron temperatures are reduced they are still in the 100s of eV range.

detachment of H^- [44, 45], no three-body recombination rates appear to have been reported for electron attachment to neutral atomic hydrogen. Several points are worth noting, firstly, the ionization cross section of H^- is quite large (peaking at around 3.5×10^{-15} cm^2) [38]. The corresponding three-body rate coefficient is then also significant and about a factor of two larger than the three-body recombination rate of electrons with protons to form neutral atomic hydrogen. However, recombination into neutral hydrogen can also proceed into excited states of the hydrogen atom and these recombination rates are large. No such channel is available for electron attachment in the H^0 case, since only one bound state of H^- is observed. Using the principle of detailed balancing and the electron impact cross-sections [44, 45], the rate coefficient for the three-body recombination computed as a function of the electron temperature is shown in Fig. 6. Given these rates, it is possible to estimate the H^- yield. Using these rates with the co-propagating model [9], it is seen that H^- generation from H^0 is possible and is dominated by three-body attachment.

For computing H^- formation, both the electron density and temperature are needed.

The former is obtained by extrapolating the electron density computed by HYADES, since, being a radiation hydrodynamics code, it cannot model the behaviour of the non-fluid-like lowest density regions. We use a simple continuity condition for the extrapolation, followed by a conical expansion of the electron emission corresponding with the experimentally measured electron angular-distribution. We note that the electron temperature is the crucial parameter. As seen in Fig. 4, even if the electron density is varied by orders of magnitude, unless the temperature is low, there is no effective electron-ion recombination.

Obtaining electron temperature in the co-propagating reference frame of the proton is difficult not only because of a number of competing processes that generate low energy electrons, but also because the low energy electron release is over an extended period of time as compared to the ion acceleration. So, the electron temperature is used as a variable parameter to evaluate the recombination reactions. The chain of electron recombination reactions of H^+ to H^0 is computed using the electron-ion recombination rates whilst the reduction to H^- was evaluated using the three-body electron attachment rates as seen in Fig. 6.

To calculate the formation of negative ions a two-step co-propagating model was used as described in [9]. Here, the first step in the calculation is to evaluate the formation of neutral atoms due to co-propagation. For each time-step, the neutral atom formation is calculated. After the neutral atoms are formed, the neutral atoms co-propagate further with electrons, leading to the formation of negative ions by the same mechanism. Since the negative ions have a very low ionization potential, collisional detachment of negative ions with electrons was taken into account. The rate equations employed were:

$$dN_0/dt = R_{1,0}(Ne, Te)\ Ne(x,t)\ N_+(x,t) \tag{1}$$

$$dN_-/dt = R_{0,-1}(Ne)\ Ne(x,t)^2\ N_0(x,t) \tag{2}$$

$$dN_0/dt = R_{-1,0}(Ne)\ Ne(x,t)\ N_-(x,t) \tag{3}$$

Where N_+, N_0 and N_- are the number of protons, neutrals and negative ions of hydrogen as a function of space and time. Ne and Te are the number density and temperature of the co-propagating electrons and $R_{x,y}$ is the conversion rate of charge state x to y. $R_{1,0}$ corresponds to electron attachment to a proton, $R_{0,-1}$ is electron attachment to hydrogen atom and $R_{-1,0}$ corresponds to electron-impact ionization of negative ions. The rate equations were then solved for different ion energies for the same co-propagating temperature and the results are shown in Fig. 3.

Carrying out the calculation for various ion energies, the relative yield of negative ions can be obtained and the simulated H^- spectrum is shown in Fig. 3. It can be seen that using the same electron temperature as in ref. [9], which successfully explained the formation of H^0 in those experiments, also provides the necessary conditions for the formations of H^- ions here. There is some discrepancy between the results of such calculations and the experimental measurement but this may be due to the fact that the same effective temperature is employed in both charge reduction steps from H^+ to

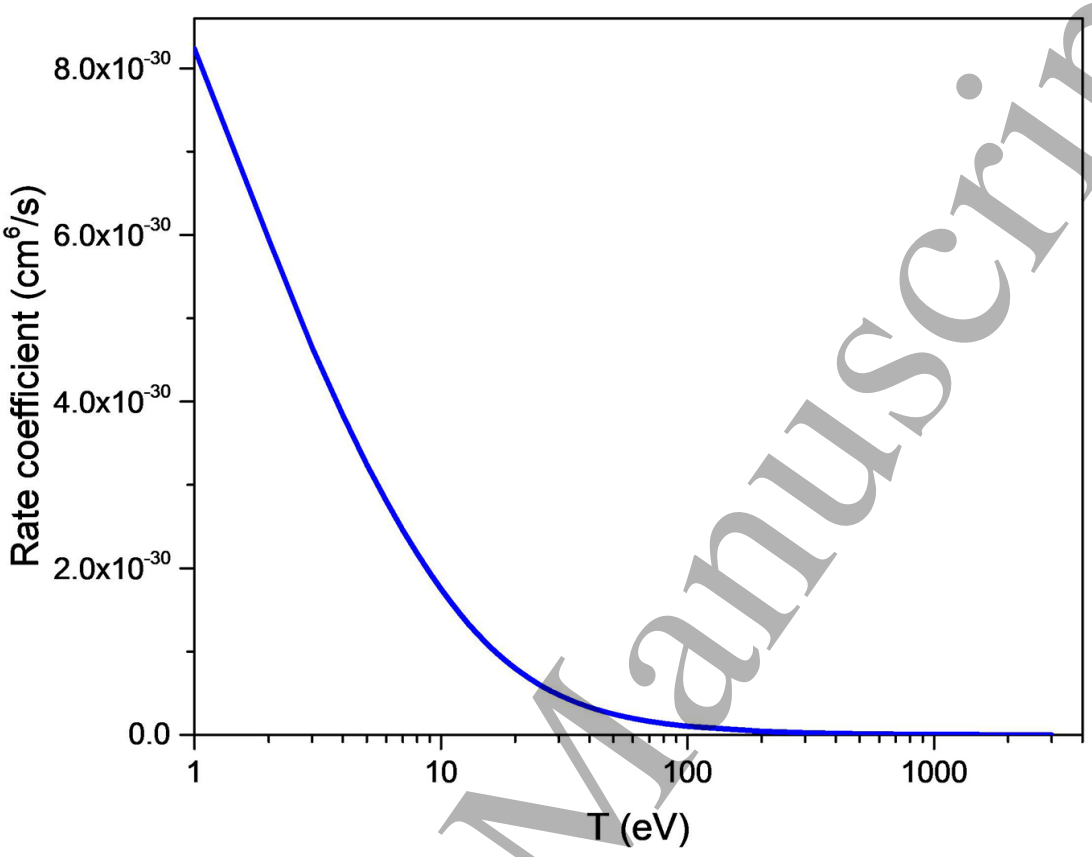

Figure 6. The three-body rate coefficient for formation of H^- as a function of electron temperature.

H^-. Given the experimental geometry, it is clear that the effective electron temperature going from H^0 to H^- should not be exactly the same as that for the subsequent H^+ to H^0 step. Small changes in the electron temperatures would improve the correlation with the experiments, however it is felt that the existing model is more robust in that it limits the number of free parameters in the model. The model anyway establishes that charge reduction and electron attachment to neutral atoms can occur in relevant numbers along the path towards the detector by a co-propagating bunch of electrons. Another possible process to form H^- is that of radiative attachment of electrons to H^0 [46] formed previously [9]. It was calculated that as the neutral atoms propagate to the detector, radiative attachment processes accounts for about 1/100 th the flux of H^- compared to that provided by three-body attachment in the co-propagating model. Isolation of this effect is therefore not feasible based on the experimental results, and may be deemed insignificant.

So, whilst negative ion formation has been reported in a few intense laser-plasma interaction experiments in the past, the arguments and simulations presented here clearly establish that the mechanism in the experiment described here is electron attachment to H^0 which has not been previously reported in any cross-beam or co-

propagating experiments.

4. Conclusion

An experimental study of ions accelerated from solid targets exposed to high contrast and high intensity laser irradiation is seen to generate fast negative ions. H^- ions up to 80 keV with a relative yield of about 0.1% compared to the proton yield are measured using gated Thomson-parabola spectrometry. Until recently, direct charge-reduction processes with electrons in ultra-short, high contrast, high-intensity laser pulses had not been demonstrated. A scheme where low-energy electrons co-propagate with the ions and continue to interact long after the ions leave the target is shown to explain the charge reduction and electron attachment to neutral hydrogen atoms to generate the negative ions observed here. For this three-body attachment, rates for the reduction of H^0 to H^- were computed and are used to evaluate the electron attachment to fast neutral atoms to form the measured H^- population. It was seen that the computed spectrum of H^- agreed well with the experiment. Intense laser-plasma interaction experiments provide an interesting environment in which to study basic atomic physics processes.

5. Acknowledgement

MK acknowledges the DST-SRC-OI grant of the Govt. of India. JC acknowledges the support by the US Department of Energy through the Los Alamos National Laboratory. Los Alamos National Laboratory is operated by Triad National Security, LLC, for the National Nuclear Security Administration of U.S. Department of Energy (Contract No. 89233218CNA000001).

References

[1] Andersen T., Physics Reports **394** 157 (2004).
[2] Tanner G, Richter K and Rost J M, Rev. Mod. Phys., **72**, 497, (2000).
[3] Faircloth D and Lawrie S., New Journal of Physics, **20**, 025077 (2018)
[4] Jayamanna K, Ames F, Bylinskii I, Lovera M, Minato B., Nucl. Instrum. Meth. Phys. Res. A **895**, 150 (2018).
[5] Bacal M and Wada M, App. Phys. Rev., **2**, 021305 (2015).
[6] Christophorou L G and Stockdale J A D, J. Chem. Phys. **48**, 1956 (1968).
[7] Van de Graff R. J., Nuc. Inst. Meth. **8** 195-202 (1960).
[8] Bin J., *et al.* Appl. Phys. Lett. **101**, 243701 (2012).
[9] Tata S. *et al.* Phys. Rev. Lett. **121**, 134801 (2018).
[10] Macchi A, Borghesi M , and Passoni M, Rev. Mod. Phys., **85**, 751 (2013).
[11] Daido H , Nishiuchi M, and Pirozhkov A S, Rep. Prog. Phys., **75**, 056401. (2012).
[12] Snavely R A , *et al.* Phys. Rev. Lett., bf 85, 2945, (2000).
[13] Hegelich M. *et al.*, Phys. Rev. Lett. **89**, 085002 (2002).
[14] Beg F N., *et al.* Phys. of Plasmas, **4**, 447-457 (1997).
[15] Kumar G. R., Pramana J. Phys., **73(1)**, 113-155 (2009).
[16] Gordienko V M., *et al.*, **44**, 2555-2568 (2002).
[17] Fuchs J., *et al.* Phys. Rev. Lett., **94**, 045004 (2005).

Direct electron attachment to fast hydrogen in 10^{-9} contrast 10^{18} Wcm^{-2} intense laser solid target interactio

[18] Kar S., *et al.* Nat. Comm., **7**, 10792 (2016).
[19] Abicht F.,*et al.* Appl. Phys. Lett., **103**, 253501 (2013).
[20] Ter-Avetisyan S., *et al.* Rev. Sci. Instrum., **83**, 02A710 (2012).
[21] Ter-Avetisyan S., *et al.* Appl. Phys. Lett., **99**, 051501 (2011).
[22] Ter-Avetisyan*et al.* Rev. Sci. Instrm., **87**, 02B134 (2016).
[23] Rajeev R., *et al.*. New J. Phys., **15**, 043036 (2013).
[24] Nakamura T., *et al.* Phys. Lett. A, **373**, 2584 - 2587 (2009).
[25] Nakamura T. et al., Phys. Plasmas 16, 113106 (2009).
[26] Volkov R V., *et al.* Pis'ma v Zhurnal Ehksperimental'noj i Teoreticheskoj Fiziki, **76**, 171-175 (2002).
[27] Chutko O V., *et al.* Appl. Phys. B, **77**, 831-837 (2003).
[28] Bagchi S., *et al.*, Phys. Rev. E, **92**, 051103 (2015).
[29] McKenna P, Neely D, Bingham R, Jaroszynski D, (ed) 2013 *Laser-Plasma Interactions and Applications* (Springer Science & Business Media).
[30] Macchi A, *Basics of Laser-Plasma Interaction: A Selection of Topics* (2019) (Springer Proceedings in Physics book series (SPPHY, volume 231).
[31] Tata S., *et al.* Rev. Sci. Instrum., **88**, 051708 (2017).
[32] Rajeev R., Rishad K P M , Madhu Trivikram T, Narayanan V, and Krishnamurthy M., Rev. Sci. Instrum., **82**, 083303 (2011).
[33] Agosteo S. et al., Nucl. Instrum. and Meth. Phys. Res. B **331**, 15 (2014).
[34] Schreiber J., Bolton, P. R. & Parodi, K., Rev.of Sci. Instrum. **87**, 071101 (2016).
[35] Lykke, K.R., Murray, K.K., Lineberger, W.C., Phys. Rev. A, **43**, 6104,(1991).
[36] Barat M., and Roncin P., J. Phys. B **25**, 2205 (1992).
[37] Hahn Y. , Rep. Prog. Phys. **60**, 691 (1997);
[38] Stier P. M. and Barn C. F., Phys. Rev. **103**, 896 (1956).
[39] Rajeev R., Thesis, 2012.
[40] Larsen J T., Lane, S M., J. Quan. Spec. Rad. Trans., **51**, 179-186 (1994).
[41] Chung H K., *et al.* High Energy Density Physics **1**, 3 (2005).
[42] Hakel P. *et al. J. Quant. Spectr. Rad. Transfer* **99**, 265 (2006).
[43] Fontes C. J. *et al. J. Phys. B* **48**, 144014 (2015).
[44] Peart B., Walton D.S., and Dolder K.T. , J. Phys. B, **3**, 1346 (1970).
[45] Pindzola, M.S., Phys. Rev. A, **54**, 3671 (1996).
[46] McLaughlin B M *et al* J. Phys. B: At. Mol. Opt. Phys. **50** 114001 (2017).